Electron microscopy study of octahedral tilt/hybridization/physical properties relationships in nickelate superlattices

Gauquelin, N.[1], Liao, Z.[2], Müller-Caspary, K.[1], Lobato, I.[3], Huijbens, M.[2], Van Aert, S.[3], Koster, G.[2], Rijnders, G.[2] and Verbeeck, J.[4]

[1] EMAT, University of Antwerp, Belgium, [2] MESA+, University of Twente, Netherlands, [3] Electron Microscopy for Materials Science (EMAT), University of Antwerp, Groenenborgerlaan 171, 2020 Antwerp, Belgium, Belgium, [4] EMAT, Electron microscopy for materials science, University of Antwerp, Groenenborgerlaan 171, 2020 Antwerp, Belgium

Rare-earth nickelate perovskites $RNiO_3$ (R being the rare earth) possess a metal-insulator transition (MIT) that is tuneable in the bulk by the size of the rare-earth atom, sitting on the A site, which influences the rotation of the NiO_6 octahedra.[1] In thin-film heterostructures, the rotation patterns can be altered by epitaxial strain. In this contribution, we will present recent results that show that the oxygen octahedral rotations of a given compound can be precisely adjusted within a broad range by combining $SmNiO_3$ with a different perovskite used as a tilt-control layer (TCL). Through scanning transmission electron microscopy (STEM), the oxygen octahedral can be visualized and measured unit cell by unit cell.[2,3] We reveal a link at the atomic-scale between a decrease of the NiO_6 tilt angles and a reduced MIT temperature, further confirmed from a simple theoretical model. In a second example using $RNiO_3$ (R=Sm, Nd) superlattices, we will demonstrate the relationship between metal-oxygen hybridization, oxygen octahedral tilt and metal-insulator transition using a combination of ABF-STEM imaging, HREELS fine structure analysis of the O K edge and structural parameter determination using statistical parameter estimation theory. A similar methodology has been applied previously to demonstrate the origin of magnetic anisotropy in STO buffered/unbuffered $La_{0.6}Sr_{0.4}MnO_3$ films deposited on $NdGaO_3$.[2,4,5]

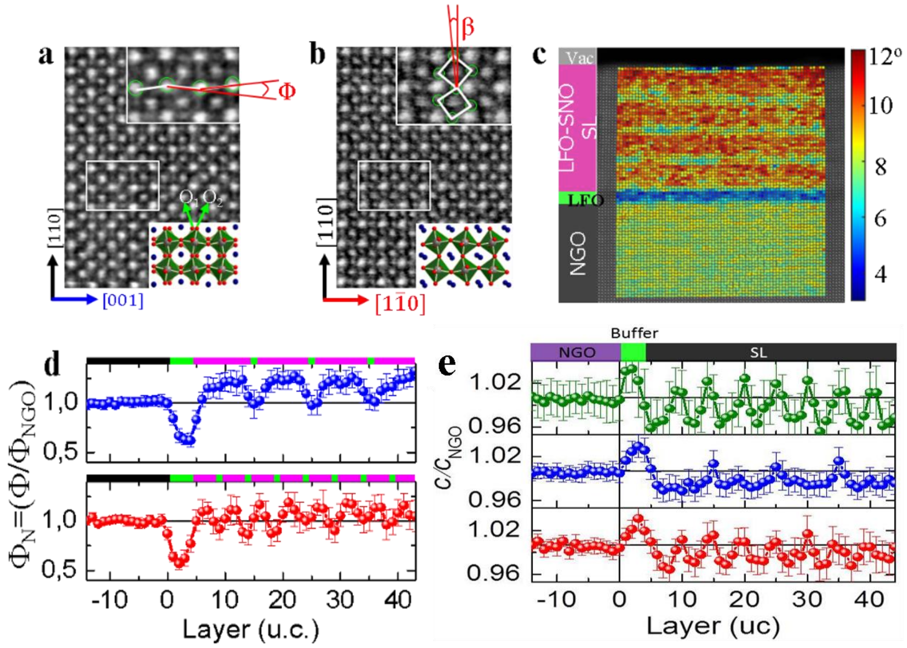

Figure 1: Atomic scale characterization of superlattices of 1 unit cell $LaFeO_3$ with n unit cells $SmNiO_3$ (n= 4, 10)(LFO1-SNOn). (a-b) Inversed contrast ABF images of LFO1-SNO4 with zone axis along [1-10] and [001] directions respectively. (c) 2D mapping of tilt angle Φ of the octahedra in LFO1-SNO10 measured with the ImageEval software[6] after statistical parameter estimation fit of the atomic positions using the StatSTEM software[7]. Each color pixel represents a local angle at a specific single A-site overlaid on the corresponding HAADF. The profile of this evolution of the octahedral titlt over the growth direction is represented in (d) for n=4 (red) and n=10(red); (e) normalized out-of-plane lattice constant (c/c_{NGO}) profiles for three superlattices: $(LFO_1/SNO_4)_{10}$ (red), $(LFO_1/SNO_{10})_4$ (blue) and $(LCO_1/LFO_4)_{10}$ (green)

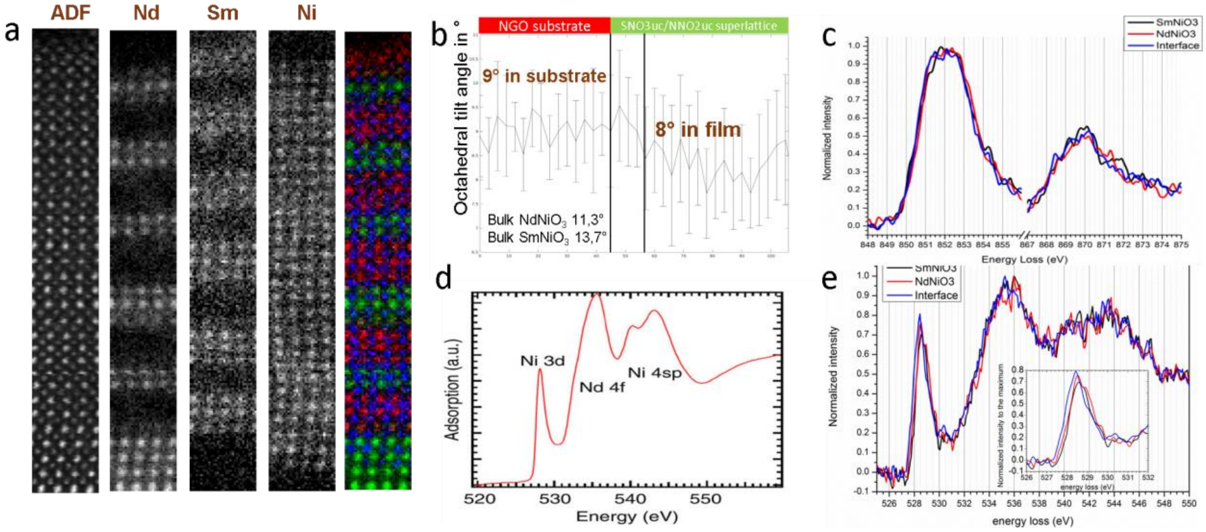

Figure 2: a) EELS elemental maps showing the good quality of the superlattice b) octahedral tilt measurements showing the strong reduction of the tilt within the first SNO layer due to oxygen octahedral coupling within the superlattice, its value is strongly reduced compare to the bulk value and constant c) EELS fine structures of the Ni $L_{2,3}$ edge showing similar electronic structure in the NNO and SNO layers d) bulk XAS spectrum at the O K edge of NNO e) EELS spectrum of the O K edge of the SNO and NNO layers within the superlattice showing and increased prepeak Ni3d-O2p indicating the increase of hybridization due to a reduced tilt angle.

[1] J. Varignon, M.N. Grisolia, J. Íæ#177;iguez, A. Barthélémy, and M. Bibes, Npj Quantum Mater. **2**, 21 (2017).

[2] Z. Liao, M. Huijben, Z. Zhong, N. Gauquelin, S. Macke, R.J. Green, S. Van Aert, J. Verbeeck, G. Van Tendeloo, K. Held, G.A. Sawatzky, G. Koster, and G. Rijnders, Nat. Mater. **15**, 425 (2016).

[3] N. Gauquelin, K.H.W. van den Bos, A. Béché, F.F. Krause, I. Lobato, S. Lazar, A. Rosenauer, S. Van Aert, and J. Verbeeck, Ultramicroscopy **181**, 178 (2017).

[4] Z. Liao, R.J. Green, N. Gauquelin, S. Macke, L. Li, J. Gonnissen, R. Sutarto, E.P. Houwman, Z. Zhong, S. Van Aert, J. Verbeeck, G.A. Sawatzky, M. Huijben, G. Koster, and G. Rijnders, Adv. Funct. Mater. **26**, 6627 (2016).

[5] Z. Liao, N. Gauquelin, R.J. Green, S. Macke, J. Gonnissen, S. Thomas, Z. Zhong, L. Li, L. Si, S. Van Aert, P. Hansmann, K. Held, J. Xia, J. Verbeeck, G. Van Tendeloo, G.A. Sawatzky, G. Koster, M. Huijben, and G. Rijnders, Adv. Funct. Mater. **27**, 1 (2017).

[6] K. Müller-Caspary, T. Mehrtens, M. Schowalter, T. Grieb, A. Rosenauer, F. F. Krause, C. Mahr, and P. Potapov, in *Eur. Microsc. Congr. 2016 Proc.* (Wiley-VCH Verlag GmbH & Co. KGaA, Weinheim, Germany, 2016), pp. 481 - 482.

[7] A. De Backer, K.H.W. van den Bos, W. Van den Broek, J. Sijbers, and S. Van Aert, Ultramicroscopy **171**, 104 (2016).

M.H., G.K. and G.R. acknowledge funding from DESCO program of the Dutch Foundation for Fundamental Research on Matter (FOM) with financial support from the Netherlands Organization for Scientific Research (NWO). J.V. and N.G. acknowledge the GOA project "Solarpaint" of the University of Antwerp for funding. The Qu-Ant-EM microscope used in this study was partly funded by the Hercules fund from the Flemish Government.